Cubatic phase for tetrapods

Ronald Blaak*
Institut für Theoretische Physik II, Heinrich-Heine-Universität, D-40225 Düsseldorf, Germany

Bela M. Mulder† and Daan Frenkel‡
FOM Institute for Atomic and Molecular Physics, Kruislaan 407, 1098 SJ Amsterdam, The Netherlands

We investigate the phase behavior of tetrapods, hard non-convex bodies formed by 4 rods connected under tetrahedral angles. We predict that, depending on the relative lengths of the rods these particles can form a uniaxial nematic phase, and more surprisingly they can exhibit a cubatic phase, a special case of the biaxial nematic phase. These predictions may be experimentally testable, as experimental realizations of tetrapods have recently become available.

I. INTRODUCTION

The simplest liquid crystalline phase is the nematic. It is a spatially homogeneous phase in which the orientations of the non-spherical component particles, e.g. rod-like or disk-like colloids, are distributed in an anisotropic fashion. More precisely, they are oriented around a preferred axis yielding a phase with macroscopic uniaxial optical anisotropy. However, this represents only the simplest form of rotational symmetry breaking. When in addition the cylindrical symmetry around the nematic director is broken, the phase that results is the so-called biaxial nematic phase. As the name biaxial suggests, there are now two preferred axes, which are mutually perpendicular. Biaxial phases can be expected if the constituent particles themselves do not have (effective) cylindrical symmetry, but are only invariant under a limited number of discrete rotations [1, 2]. Biaxial phase may also appear in mixtures of rod-like and disk-like particles. Each of the two components individually will form uniaxial nematic phases at sufficiently high densities. When mixed they will do the same, but their mutual interaction is such that the preferred orientation axis for the rods is perpendicular to that of the disks [3, 4, 5, 6].

This still does not exhaust all possibilities for spatially homogenous liquid-crystalline phases. Frenkel [7] proposed that particles consisting of three identical rods, connected at right angles at their center, should form a stable high-density phase with cubic orientational symmetry. This liquid crystalline phase is referred to as a cubatic phase. It is a special case of the general biaxial phase, since there are now three mutually perpendicular axes of symmetry that are equivalent.

This model has subsequently been generalized to cross-like particles ("Onsager crosses"), in which the three rods can have unequal lengths [8]. These particles show a surprisingly rich phase behavior. Not only do they form a cubatic phase in the case that the three rods have approximately equal lengths, but they can also show rod-like and plate-like behavior by forming uniaxial nematic phases if one, respectively two, rods are dominant in determining the shape of the particle. Moreover, at higher densities, these uniaxial nematic phases become unstable and different types of biaxial nematic phases are formed.

Unfortunately these lower-symmetry liquid-crystalline phases have, thus far, not been observed in experiment. The main problem seems to be that, unlike the rod-like colloidal particles that form nematics, cross-like particles that are both rigid and sufficiently monodisperse could not be made in a sufficient quantities to allow a systematic study of their phase behavior. In particular the cubatic phase has not yet been observed in experiments, although simulations have suggested that a phase with this symmetry may exist in a system of disk-like particles [9].

Recently, however, Alivisatos *et al.* have reported the synthesis of colloidal CdTe tetrapods [10]. These particles could be made with a high yield and with well-controlled nanoscale dimensions. The experimental tetrapods consists of a small crystalline body from which four arms grow under tetrahedral angles. Since these arms are also crystalline, the tetrapods are fairly rigid and, with a suitably chosen solvent (and proper steric stabilization), should behave as rigid hard-core particles.

In this paper we consider the liquid crystalline behavior of tetrapods. For simplicity we work in the Onsager limit of large aspect ratios and only take into account a hard-core interaction. We assume that the particles are monodisperse, but we treat all possible combinations of relative lengths for the arms of the tetrapod. We focus here on a bifurcation analysis, which gives us an upper limit to the stability of the isotropic phase and yields an indication of the nature of the more stable liquid crystalline phases. Using this analysis, we argue that the tetrapods of ref. [10] should, under certain conditions, form cubatic phases.

In section II we justify the main assumptions of the model and derive an expression for the Helmholtz free energy. We make use of rotation matrix elements, of which the main properties and conventions are briefly

*Electronic address: blaak@thphy.uni-duesseldorf.de
†Electronic address: mulder@amolf.nl
‡Electronic address: frenkel@amolf.nl

described in the appendix. In section III we perform the stability analysis of the isotropic phase and interpret the results, and conclude with a discussion of the main results in section IV.

II. THE MODEL

To analyze the phase behavior of hard tetrapods, we need expression for the free energy of this system. In general, this is an intractable problem. However, for tetrapods with sufficiently slender arms we can make the same assumptions that were introduced by Onsager in the context of the isotropic-nematic transition of thin hard rods [11]. Onsager showed that for a fluid of particles with large (strictly speaking, infinite) length-to-width ratio, the excess free energy can be truncated at the second virial coefficient level. In the case of hard-core interactions this is equivalent to assuming that if one randomly places particles with a given density in space, the probability that three particles mutually overlap is negligibly small.

Although we have assumed large aspect ratios for the arms that constitute a tetrapod, it is not immediately obvious that the second virial approximation is valid. However, since tetrapods are essentially objects with an open structure and consist of four connected rod-like particles, one would expect that if two particles overlap with each other this is mainly due to a single arm of one particle that overlaps with a single arm of the other particle.

The validity of this plausibility argument is confirmed explicitely for Onsager crosses with three equally long arms in the isotropic phase [12]. In a detailed analysis it is shown that for a length-to-width ratio of about one thousand the probability that, under the constraint that two particles overlap, more than a single pair of the arms are overlapping, is less then a percent and decreases for increasing aspect ratios. In other words, in the limit of large aspect ratios one can describe the particle-particle interaction in terms of independent pairs of arm-arm interactions only.

What Onsager showed for elongated particles in the isotropic phase is that the asymptotic limit of the third virial coefficient B_3 can be expressed in terms of the second virial coefficient and the aspect ratio by $B_3 = B_2^2\mathcal{O}(D/L\log(L/D))$ [11]. This has been confirmed by the calculation of virial coefficients for long spherocylinders [13]. The fourth and fifth virial showed a similar dependence $B_n = B_2^{(n-1)}\mathcal{O}(D/L)$. Since the interaction between Onsager crosses in leading order is determined by single rod-rod interactions the same behavior should be observed for Onsager crosses, as indeed is found, provided aspect ratios are of the order thousand [12]. In addition, the main contribution to the higher virial coefficients stems from the so-called ring diagrams, which would lead to same scaling behavior for higher order virial coefficients. Hence corrections to the free energy due to the simultaneous interaction of three or more particles is an order D/L smaller than the second virial contribution and can therefore be neglected in the limit of infinite aspect ratios.

In summary then, the assumptions that virial expansion of the free energy can be truncated at the second-virial level and that the interaction between particles can be considered as a sum of pair interactions between the "arms" of the particles, become exact in the limit of infinite aspect ratios. For large but finite aspect ratios, these assumptions should constitute excellent approximations

The truncation of the virial series leads to the following free-energy functional for homogeneous systems

$$\begin{aligned}\beta f[\psi] = \beta\hat{f} + \int d\Omega\psi(\Omega)\ln\psi(\Omega) \\ + \frac{1}{2}\rho\int d\Omega_1\int d\Omega_2\psi(\Omega_1)\psi(\Omega_2)\mathcal{E}(\Omega_1,\Omega_2)\end{aligned} \tag{1}$$

Here f is the Helmholtz free energy per particle, which is a functional of ψ the orientational distribution function (ODF). This ODF is a measure for the fraction of particles with an orientation Ω, which is shorthand for the three Euler angles $(\alpha,\beta\gamma)$ required to specify an arbitrary orientation in a fixed reference frame, and is normalized to unity. $\beta = (k_BT)^{-1}$ is the inverse temperature, ρ the number density and $\hat{f}$ the ideal gas term that does not explicitly depend on the ODF. The second term corresponds to the orientational entropy, while the third term is associated to the translational entropy through the kernel $\mathcal{E}(\Omega_1,\Omega_2)$ describing the over space integrated interaction of two tetrapods with orientations Ω_1 and Ω_2.

The interaction of hard-core objects is taken into account via the excluded volume $\mathcal{E}(\Omega_1,\Omega_2)$. This volume, is defined as the volume around particle 1 (with orientation orientations Ω_1) that is inaccessible to particle 2 (with orientation orientations Ω_2). For two slender particles, with lengths L_1 and L_2 and diameters D_1 and D_2 respectively the excluded volume is, to leading order, given by

$$L_1L_2(D_1+D_2)|\sin\gamma|, \tag{2}$$

where γ is the angle between the long axes of the particles. Corrections to this expression are of order D/L. Since we are mainly interested in the limit of large aspect ratios, we restrict ourselves to the leading order only.

In the case of tetrapods the excluded volume is, of course, more complicated. First of all we now have four rod-like arms. We will assume that the arms can be approximated by cylinders with identical diameter D, but possibly different lengths L_i, where $i = 1,2,3,4$. With the assumption that the arms of tetrapods, whilst connected, interact independently, the excluded volume of two tetrapods becomes a sum over the pairwise excluded volumes of the arms

$$\mathcal{E}(\Omega_1,\Omega_2) = \sum_{i,j} 2L_i^{(1)}L_j^{(2)}D|\sin\gamma_{ij}^{12}|, \tag{3}$$

where the superscript refers to the particle and the subscript to the arm of the tetrapod, hence γ_{ij}^{12} is the angle

between the ith and jth arm of particle 1 and 2 respectively. For the isotropic phase this leads to a simple expression for the second virial coefficient B_2. It is equal to half the excluded volume averaged over all orientations, as it is simply equal to the sum of second virials for all pairs of rods

$$B_2 = \frac{\pi}{4} D \left(\sum_i L_i \right)^2 . \tag{4}$$

We note that we can expand any ODF depending on Ω in terms of a linear combination of Wigner rotation matrix elements $\mathcal{D}^l_{m,n}(\Omega)$. In what follows, we adopt the convention used by Brink and Satchler in the description of the Wigner matrices [14].

In order to make use of the free energy functional (1), we need to rewrite the interaction (3) in terms of these functions. To this end, we introduce an arbitrary reference orientation of a tetrapod. We denote the directions of the arms with length L_i of the reference tetrapod by the unit-vectors $\hat{e}_i$. For simplicity we assume that $\hat{e}_1 = \hat{z}$ is the positive z-direction and $\hat{e}_2$ is lies in the xz-plane with a positive x-component. Since by definition the mutual directions are under tetrahedral angles this fixes all directions.

This allows us to interpret the orientation Ω of a particle, as the one we would obtain if we take the reference particle and rotate it over the Euler angles denoted by Ω. Additionally we can also interpret Ω as the actual rotation matrix, so the directions of the arms of a particle become $\Omega\hat{e}_i$. Finally, we introduce the rotations g_i, such that $\hat{e}_i \equiv g_i\hat{z}$. Note that these rotations g_i are not uniquely defined, since only two of the Euler angles are required in order to satisfy the restriction. However, this has no effect on the final result.

It is obvious that the excluded volume (3) of two tetrapods cannot depend on both orientations independently, but only on the relative orientation $\Omega_1^{-1}\Omega_2$. Hence we can rewrite the excluded volume as

$$\begin{aligned} \mathcal{E}(\Omega_1^{-1}\Omega_2) &\equiv \mathcal{E}(\Omega_1, \Omega_2) \\ &= \sum_{i,j} 2L_i^{(1)} L_j^{(2)} D |\Omega_1 \hat{e}_i^{(1)} \times \Omega_2 \hat{e}_j^{(2)}| \\ &= \sum_{i,j} 2L_i^{(1)} L_j^{(2)} D |\hat{z}^{(1)} \times g_i^{-1}\Omega_1^{-1}\Omega_2 g_j \hat{z}^{(2)}|. \end{aligned} \tag{5}$$

With the aid of this form we can now expand the excluded volume in terms of rotation matrix elements $\mathcal{D}^l_{m,n}(\Omega)$, by introducing the expansion coefficients $E_{l,m,n}$

$$\mathcal{E}(\Omega) \equiv \sum_{l,m,n} E_{l,m,n} \mathcal{D}^l_{m,n}(\Omega), \tag{6}$$

where $l = 0, 1, \cdots, \infty$, and $-l \leq m, n \leq l$. Strictly speaking, the rotation matrix elements also defined for half-integer "spin" values. However, for reasons of symmetry these can be omitted [14].

The expansion coefficients can be evaluated by using the orthogonality relation (A2) for the rotation matrix elements

$$E_{l,m,n} = \frac{2l+1}{8\pi^2} \int d\Omega \mathcal{D}^{l\,*}_{m,n}(\Omega) \mathcal{E}(\Omega). \tag{7}$$

Substituting the expression (5) and changing the integration variables we get

$$\begin{aligned} E_{l,m,n} &= \frac{2l+1}{8\pi^2} 2D \sum_{i,j} L_i L_j \int d\Omega \mathcal{D}^{l\,*}_{m,n}(g_i \Omega g_j^{-1}) |\hat{z}^{(1)} \times \Omega \hat{z}^{(2)}| \\ &= \frac{2l+1}{8\pi^2} 2D \sum_{p,q} \left(\sum_i L_i \mathcal{D}^{l\,*}_{m,p}(g_i) \right) \left(\sum_j L_j \mathcal{D}^l_{n,q}(g_j) \right) \int d\Omega \mathcal{D}^{l*}_{p,q}(\Omega) |\sin\beta| \end{aligned} \tag{8}$$

where we made use of the symmetry relation (A1) and closure relation (A3) and replaced the cross product by its representation in Euler angles $|\sin\beta|$.

In order for the integral to be non-zero, it is required that both indices of the rotation matrix element are zero. This is a special case for which the function reduces to a Legendre polynomial $\mathcal{D}^l_{0,0}(\Omega) = P_l(\cos(\beta))$. By introducing the following shorthand notations

$$E_{l,m} \equiv \sum_i L_i \mathcal{D}^l_{m,0}(g_i) \tag{9}$$

$$\mu_l \equiv \frac{2l+1}{2} \int_0^\pi d\beta P_l(\cos\beta) \sin^2\beta \tag{10}$$

the expansion coefficients of the excluded volume can be written in a compact form as

$$E_{l,m,n} = (2D)\mu_l E^*_{l,m} E_{l,n}. \tag{11}$$

The integral that remains can be readily evaluated (See [15] Eq. 7.132.1) and is only non-zero for even value of l

$$\begin{aligned} \mu_{2l} &= -\frac{\pi(4l+1)}{(l+1)(2l-1)2^{4l+2}}\binom{2l}{l}^2 \\ \mu_{2l+1} &= 0. \end{aligned} \tag{12}$$

Finally we introduce another shorthand notation by using the kernel (3) as a functional acting on an arbitrary function $\psi(\Omega)$

$$\mathcal{E}[\psi](\Omega) \equiv \int d\Omega' \mathcal{E}(\Omega'^{-1}\Omega)\psi(\Omega'). \tag{13}$$

In particular we allow it to operate on a rotation matrix element. Using the expansion (6) and the properties (A1) and (A3) this can be manipulated to yield

$$\mathcal{E}[\mathcal{D}^l_{m,n}] = \sum_p E_{l,n,p}\mathcal{D}^l_{m,p}(\Omega). \tag{14}$$

Note that this generates a linear combination of rotation matrix elements with the same value for l and m. In other words each set $\mathcal{D}^l_{m,n}$ with $n = -l, \cdots, l$ forms a subset of functions that is invariant under the functional operator of the excluded volume. We can go one step further by evaluating eigenfunctions of the excluded volume. Using the special form of the coefficients (11), one can easily check that for each combination of l and m at most a single eigenvector χ^l_m exist with a non-zero eigenvalue λ_l

$$\chi^l_m(\Omega) = \sum_p E_{l,p}\mathcal{D}^l_{m,p}(\Omega) \tag{15}$$

$$\lambda_l = (2D)\mu_l \sum_p E^*_{l,p}E_{l,p}. \tag{16}$$

Note that the eigenvalue is independent of m and in special cases also might become zero as for instance for odd values of l.

III. BIFURCATION ANALYSIS

The thermodynamically stable phase of our model, is described by the ODF that minimizes the free energy (1). Usually this free energy is not known exactly and one uses a truncated expansion as an approximate function. There is however one exception: the isotropic phase. In the limit of infinite dilution, particles do not interact and therefore each orientation has the same probability, hence the ODF is merely a constant.

With the aid of a bifurcation analysis we can determine an upper limit to the stability of the isotropic phase. To this end, we make an expansion of the ODF around the stable isotropic solution. Rather than inserting this into the free energy (1), we use this to find solutions of the stability equation that is obtained as the functional derivative of the free energy with respect to the ODF

$$\frac{\delta}{\delta\psi(\Omega)}\left\{\beta f[\psi] - \lambda\int d\Omega\psi(\Omega)\right\} = 0, \tag{17}$$

where λ is a Lagrange multiplier to take care of the proper normalization of the ODF. Evaluating this expression and using the definition (13) this gives us

$$\ln(\psi(\Omega)) + \rho\mathcal{E}[\psi](\Omega) = \lambda. \tag{18}$$

For both the ODF ψ and number density ρ we take the formal expansion in a small parameter ϵ

$$\psi = \psi_0 + \epsilon\psi_1 + \epsilon^2\psi_2 + \cdots \tag{19}$$

$$\rho = \rho_0 + \epsilon\rho_1 + \epsilon^2\rho_2 + \cdots. \tag{20}$$

Here we use $\psi_0 = \frac{1}{8\pi^2}$ as the ODF for the isotropic phase. By inserting these expansions in the stability equation (18) and grouping terms for each power in ϵ, we obtain the bifurcation equations. By solving these we can find the lowest density ρ_0 at which a symmetry breaking mode exists that lead to a lower free energy than that of the isotropic phase. In the case of a non-zero value for ρ_1 this is sign of a first order phase transition at a lower density and hence ρ_0 is the upper limit for the meta-stability of the isotropic phase.

The zeroth-order bifurcation equation merely states that the isotropic solution $\psi = \psi_0$ is a solution of the stationarity equation. The first order bifurcation has the form of an eigenvalue problem

$$\frac{\psi_1}{\psi_0} + \rho_0\mathcal{E}[\psi_1] = 0, \tag{21}$$

where we have already eliminated the constant contributions. Since we are interested in a non-trivial solution that leads to the lowest possible positive value of ρ_0, we only need to consider linear combinations of eigenfunctions (15). In particular we need to find the one that has the largest absolute value among all negative eigenvalues.

One can show that, for the case of tetrapods, there are only two eigenvalues that can fulfill that requirement, namely the ones corresponding to $l = 2$ and $l = 4$

$$\lambda_2 = -\frac{\pi^3}{6}DL^2(4R^2 - 1) \tag{22}$$

$$\lambda_4 = -\frac{\pi^3}{1296}DL^2(80R^2 + 1). \tag{23}$$

For practical purposes we used here $L = \sum_i L_i$, and $R^2 = (\sum_i L_i^2)/L^2$. Since $\lambda_2 = \lambda_4$ for $R^2 = \frac{31}{112}$ and by construction $\frac{1}{4} \leq R^2 \leq 1$, we need to distinguish two types of tetrapods. The ones with $R^2 > \frac{31}{112}$ for which we need to consider modes related to $l = 2$ and the ones with $R^2 < \frac{31}{112}$ for which the modes with $l = 4$ are the important ones. For the special case $R^2 = \frac{31}{112}$ we would

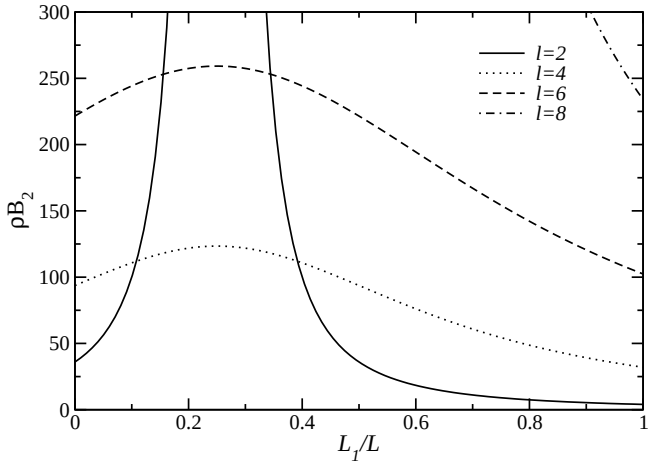

FIG. 1: The density at which the isotropic phase becomes unstable with respect to different modes characterized by l for a subset of particles with equal volume and arm lengths $L_2 = L_3 = L_4 = (L - L_1)/3$. The solid line ($l = 2$) denotes the isotropic-nematic instability and the dotted line ($l = 4$) indicates the isotropic-cubatic instability.

actually need to consider combinations of both, which makes the analysis somewhat more involved, but since this is not going to lead to new insights we will not treat it separately.

As an illustration we show in Fig. 1 the location of the four lowest instabilities of the isotropic phase for a specific class of particles, i.e. those for which $L_2 = L_3 = L_4 = (L - L_1)/3$. This set includes the fully symmetric tetrapod ($L_1/L = 1/4$) and a limiting tetrapod with only a single arm ($L_1/L = 1$). Note that the volume of each particle is the same $v = (\pi/4)D^2L$, but the density at which the isotropic phase becomes unstable for the symmetric tetrapod is approximately thirty times higher than that of a tetrapod with a single arm. The volume fraction $\phi = \rho v$, however, is proportional to D/L, which means that in the limit of large aspect ratios the transition takes place at small volume fractions.

Although we now know the upper limit to the stability of the isotropic phase, we do not yet know which are the symmetry breaking modes. To find these, we need to perform a second order bifurcation analysis, i.e. solve the equation

$$\frac{\psi_2}{\psi_0} - \frac{1}{2}\left(\frac{\psi_2}{\psi_0}\right)^2 + \rho_0\mathcal{E}[\psi_2] + \rho_1\mathcal{E}[\psi_1] = -\int d\Omega \frac{\psi_1^2}{2\psi_0^3} \quad (24)$$

employing the general solution of the first order bifurcation equation given by (21)

$$\psi_1(\Omega) = \sum_m c_m \chi_m^l(\Omega), \quad (25)$$

where the c_m are some complex constants and l is either 2 or 4. Substitution in the second-order bifurcation equation (24), multiplying with χ_n^{l*} and integrating over the orientation Ω, gives us a set of coupled non-linear equations in the coefficients c_m and constant ρ_1

$$\rho_1\lambda_l c_n \int d\Omega \chi_n^{l*}\chi_n^l = \frac{1}{2\psi_0^2}\int d\Omega \chi_n^{l*}\psi_1^2. \quad (26)$$

We can also extract the value of ρ_1, if we use the complete function ψ_1^* in stead of χ_n^{l*}

$$\rho_1 = \frac{1}{2\lambda_l\psi_0^2}\frac{\int d\Omega\psi_1^3}{\int d\Omega\psi_1^2}. \quad (27)$$

It is important to realize that there is a restriction on ρ_1. The reason is that a non-zero value of ρ_1 is associated with a first order phase transition and that in order to follow the solution towards lower densities we need a non-positive value, hence $\rho_1 \leq 0$.

Let us now consider the case $R^2 > \frac{31}{112}$ with $l = 2$ in the preceding equations. The set of equations (26) can be solved analytically and yields only a single non-trivial solution, which is degenerate since all rotations of a solution are also solutions of the set of equations. For a conveniently chosen reference frame the solution is

$$\psi_1(\Omega) = c_0\chi_0^2(\Omega) \quad (28)$$

It bifurcates at a reduced density

$$\rho_0 B_2 = \frac{12}{4R^2 - 1}. \quad (29)$$

Note that in the limit of a single arm ($R^2 = 1$) this reduces to the correct result for uniaxial rod-like particles. This particular solution is invariant under rotations about the z-axis, and hence one can expect that the system shows a phase transition from an isotropic to an uniaxial nematic phase. Inserting the solution in the expression (27) for ρ_1 we obtain

$$\begin{aligned}\rho_1 =& \frac{-\pi^3 D c_0}{14\psi_0^2\lambda_2^2}[L_1 + L_2 - L_3 - L_4]\times \\ & [L_1 - L_2 + L_3 - L_4][L_1 - L_2 - L_3 + L_4].\end{aligned} \quad (30)$$

From this result it follows that if the sum of the lengths of two arms equals the sum of the length of the two remaining arms we find $\rho_1 = 0$. These special particle configurations could therefore possibly lead to a continuous phase transition and be the source of a biaxial phase. Whether this is scenario really applies, cannot be determined from this analysis. One could resolve this issue either by solving higher order bifurcation equations or by a full numerical minimization of the free energy. This falls outside the scope of the present paper. For other particle configurations the requirement of non-positive values for ρ_1 will fix the sign of the coefficient c_0, which can be positive or negative, and hence fully determine the solution (29), because the magnitude will only depend on the choice of normalization.

Similar to the case for Onsager crosses [8], we can interpret this phenomenon in terms of rod-like and disk-like

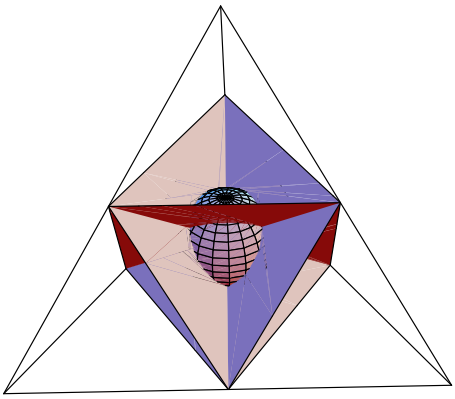

FIG. 2: Phase diagram of the nature of symmetry breaking modes leading to the instability of the isotropic phase. Each point inside the tetrahedron corresponds to a given shape of the tetrapod. A vertex corresponds to a single arm, the opposite plane to a tetrapod with three arms. For particles inside the sphere a cubatic phase is expected, outside the sphere a nematic phase which is either rod-like, if it contains a vertex, or platelet-like if it does not. Both species are separated by planes denoting the particles that might have a continuous phase transition and show biaxial behavior.

behavior. For each of the four arms of the tetrapod, we can determine the nematic order parameter, which is defined as the average value of $\frac{3}{2}\cos^2(\theta)-\frac{1}{2}$ with θ the angle between the nematic axis and the direction of the arm. It can be shown that, up to a positive normalization factor, this is proportional to $c_0(4L_i-L)/3$ for all arms. Making use of permutations of arms it follows that for positive values of c_0 the longest arm has the largest nematic order, while for negative c_0 it would be the shortest arm. A special limit of the former, is the case where L_1 is much larger than the other three. It is obvious that for such particles this longest arm will dominate the behavior and the tetrapod behaves as a single rod-like particle. The other extreme occurs when L_1 is much smaller than the other three. In that case the competition among those three arms does not allow any of them to dominate and there is a preference for them to be perpendicular to the nematic axis and, as in the case of disks, it is the smallest dimension that determines the orientation of the particle.

The set of equations (26) can also be solved for the case of $R^2 < \frac{31}{112}$, but then we need to put $l = 4$ in the equations (25)-(27). The bifurcation density can easily be determined from the proper eigenvalue (23)

$$\rho_0 B_2 = \frac{2592}{80R^2+1}. \tag{31}$$

But instead of having a single family of solutions that solve the equations (26), we now have two. The first family corresponds again to a uniaxial nematic phase for which

$$\psi_1(\Omega) = c_0\chi_0^4(\Omega) \tag{32}$$

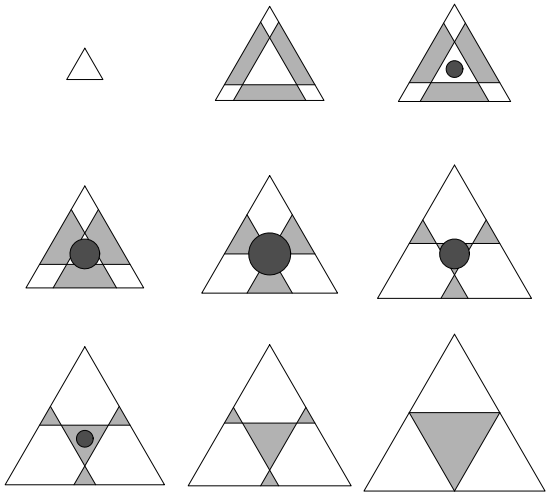

FIG. 3: Cross-sections of the phase diagram for constant value of l_i, from left to right, top to bottom for decreasing values. The dark circular areas correspond to the cubatic solution, the light and white areas to the two types of nematic solutions, being rod- and disk-like respectively.

is the particular solution invariant under rotations about the z-axis, and $c_0 < 0$ in order for ρ_1 to be negative. Contrary to the previous case c_0 does not change sign.

A particular solution of the second family of solutions is given by

$$\psi_1(\Omega) = c_0\left\{\chi_0^4(\Omega) + \frac{5}{14}\left(\chi_4^4(\Omega)+\chi_{-4}^4(\Omega)\right)\right\}. \tag{33}$$

This solution is only invariant under discrete rotations over $\pi/2$ about the x-, y-, and z-axes. It therefore corresponds to the cubic symmetry group and hence to a cubatic phase. Also in this case, the constraint on ρ_1 results in a negative value for c_0.

This analysis allows us to sketch a tentative phase diagram (see Figure 2). In this a schematic figure, we indicate the nature of the symmetry-breaking modes that lead to the instability of the isotropic phase. We can characterize the particle shape by the normalized values $l_i = L_i/L$ with the constraint $l_1 + l_2 + l_3 + l_4 = 1$. Each possible particle shape, i.e. combination of relative lengths of the arms, corresponds to a point inside a tetrahedron, which is the projection of the 4-dimensional "shape" space. A vertex of the tetrahedron represents the limit of a tetrapod with only a single arm, the triangular plane opposite to the vertex contains all particle shapes for which that same arm has zero length while the remaining three arms have non-zero lengths. In Figure 3, we have made cross-sections corresponding to planes with constant value for one of the l_i.

Nine distinct regions can be identified: a spherical region corresponding to $R^2 \leq \frac{31}{112}$, where there are two modes that lead to the instability of the isotropic phase, one of which yields the cubatic solution. In Figure 3 these regions are indicated as the dark circular areas. Outside

these regions, we find the particles for which there is only a mode with uniaxial symmetry that makes the isotropic phase unstable. There are four equivalent areas close to a vertex, shown as white in Figure 3, that represent tetrapods where the solution (28) has a positive sign, and four equivalent areas, indicated by light gray in Figure 3, where the solution has a negative sign. They are separated by the planes(lines) leading to "biaxial" particles.

IV. DISCUSSION

The present work suggests that the availability of nanocrystalline tetrapods with a well controlled size and shape [10], may make it possible to observe cubatic liquid crystalline phases in experiments. Of course, the present "Onsager-style" analysis only becomes exact in the limit of very slender, rigid arms. Within this approximation, we have determined the upper limit to the stability of the isotropic phase by means of a bifurcation analysis. In addition, we have determined the nature of the fluctuations that cause the instability.

Roughly speaking we can distinguish two types of tetrapods, the ones for which the arms have approximately the same lengths and the ones where one or more arms are significantly longer than the others. For the first group the isotropic phase becomes unstable with respect to a distortion with either nematic or cubatic symmetry, while for the second group only a nematic symmetry comes into play.

In general the transitions will be first order since we obtained a non-zero value of the first order shift in density ρ_1 along the bifurcating solutions, indicating the presence of a v.d. Waals loop. An exception might be formed by the particles located in the planes in Figure 2. Although the results of the bifurcation analysis cannot guarantee that the symmetry of the fluctuations that lead to the instability will also be the symmetry of the more stable phase, the experience in a similar study of Onsager crosses has shown that the bifurcation analysis has a high predictive value [8]. In addition, it also strongly indicates that a system of tetrapods with approximately identical arms will have an isotropic to cubatic phase transition, which in principle could be verified by a full minimization of the Helmholtz free energy functional.

Based on the results of the Onsager crosses, we predict that at higher densities a system of tetrapods will undergo additional transitions to phases with yet lower symmetry, ultimately arriving at the phase where only arms with identical lengths are aligned. In particular three intermediate phases might appear that are invariant under 2-fold, 4-fold, and 6-fold rotations from the cubic group. In some cases these phases could actually preempt the isotropic-to-nematic or isotropic-to-cubatic phase transition. This is most likely to happen for particle shapes close to the planes and/or surface that separate the different regions in the phase diagram. A full numerical free-energy minimization would be required to confirm the existence of these phases and to ascertain whether a transition from isotropic phase to any of these four phases is possible.

The formation of a cubatic phase even for fully symmetric tetrapods may seem surprising. Naively, one might expect to observe a "tetrahedratic" liquid crystalline phase. The reason why the latter phase does not appear here is related to the fact that in the Onsager approximation presented here the arms of a particle effectively interact independently with those of other particles. Essentially we are therefore insensitive to the details on how the arms are connected. Although the relative orientation of the arms within each particle is fully accounted for, we cannot specify that the arms are connected end-on. The same results would therefore be obtained for particles in which the four rods were connected at their mid-points. Such particles would in fact have cubic symmetry and are hence are unable to form a phase with tetrahedral symmetry.

The results presented here are only valid in the limit of infinite aspect ratios. For finite aspect ratios we expect two types of corrections: (i) contributions due to simultaneous overlap of three or more arms and (ii) dependencies on the detailed construction of the particles. In practice, one would presumably require aspect ratios of the order one thousand or more in order to make these corrections negligible (see Ref. [8]). Nevertheless one could expect that our qualitative findings remain valid even for smaller aspect ratios, as is the case for single rods. The fact that particles might not be perfectly monodisperse is probably not a problem, since there is a rather broad range of particle shapes that gives rise to the cubatic instability of the isotropic phase. However, finite aspect ratios imply that also non-homogeneous phases should be considered, in which the isotropic-to-cubatic transition might be preempted by crystallization. Finally, there may be kinetic limitations to the formation of cubatic phases of tetrapods, as the tetrapods are likely to become entangled at high densities, which could lead to kinetically arrested glass-like phases.

APPENDIX A: ROTATION MATRIX ELEMENTS

Here we list the main properties of the rotation matrix elements. For a more extended discussion we refer the reader to [14].

A rotation $\Omega = (\alpha, \beta, \gamma)$ is obtained by successive rotations of angles α, β, and γ about the z-, y-, and z-axis respectively. The invariant measure of the rotation is given by $d\Omega = \sin(\beta) d\alpha d\beta d\gamma$, with $\alpha, \gamma \in [0, 2\pi]$ and $\beta \in [0, \pi]$.

Symmetry relation

$$\mathcal{D}^{l\,*}_{n,m}(\Omega) = \mathcal{D}^{l}_{m,n}(\Omega^{-1}) \tag{A1}$$

Orthogonality relation

$$\int d\Omega \mathcal{D}^{l',*}_{m',n'}(\Omega) \mathcal{D}^{l}_{m,n}(\Omega) = \frac{8\pi^2}{2l+1} \delta_{l,l'} \delta_{m,m'} \delta_{n,n'} \tag{A2}$$

Closure relation

$$\mathcal{D}^l_{m,n}(\Omega_2\Omega_1) = \sum_{p=-l}^{l} \mathcal{D}^l_{m,p}(\Omega_2)\mathcal{D}^l_{p,n}(\Omega_1) \qquad \text{(A3)}$$

[1] M. J. Freiser, Phys. Rev. Lett. **24**, 1041 (1970).
[2] B. Mulder, Phys. Rev. A **39**, 360 (1989).
[3] R. Alben, J. Chem. Phys. **59**, 4299 (1973).
[4] A. Stroobants and H. N. W. Lekkerkerker, J. Phys. Chem. **88**, 3669 (1984).
[5] P. J. Camp, M. P. Allen, P. G. Bolhuis, and D. Frenkel, J. Chem. Phys. **106**, 9270 (1997).
[6] F. M. van der Kooij and H. N. W. Lekkerkerker, Phys. Rev. Lett. **84**, 781 (2000).
[7] D. Frenkel, in *Liquids, Freezing and the Glass Transition*, edited by J. P. Hansen, D. Levesque, and J. Zinn-Justin (North-Holland, Amsterdam, 1991), pp. 689–762.
[8] R. Blaak and B. M. Mulder, Phys. Rev. E **58**, 5873 (1998).
[9] J. A. C. Veerman and D. Frenkel, Phys. Rev. A **45**, 5632 (1992).
[10] L. Manna, D. J. Milliron, A. Meisel, E. C. Scher, and A. P. Alivisatos, Nature Materials **2**, 382 (2003).
[11] L. Onsager, Ann. (N.Y.) Acad. Sci. **51**, 627 (1949).
[12] R. Blaak and B. M. Mulder, Mol. Phys. **94**, 401 (1998).
[13] D. Frenkel, J. Phys. Chem. **91**, 4912 (1987), erratum: J. Phys. Chem. **92**, 5314 (1988).
[14] D. M. Brink and G. R. Satchler, *Angular Momentum* (Oxford University Press, Oxford, 1968), 2nd ed.
[15] I. S. Gradshteyn and I. M. Ryzhik, *Table of Integrals, Series, and Products* (Academic Press, San Diego, 2000), 6th ed.